Mucoadhesive gellan gum/poly(2-ethyl-2-oxazoline) films for ocular delivery of pilocarpine hydrochloride

Journal of Drug Delivery Science and Technology 104 (2025) 106492

Contents lists available at ScienceDirect

Journal of Drug Delivery Science and Technology

journal homepage: www.elsevier.com/locate/jddst

Mucoadhesive gellan gum/poly(2-ethyl-2-oxazoline) films for ocular delivery of pilocarpine hydrochloride

Guzel K. Abilova [a,**], Shamil F. Nasibullin [b], Kuanysh Ilyassov [a], Aslan N. Adilov [a], Marzhan K. Akhmetova [a], Rouslan I. Moustafine [b], Yesset T. Muratov [c], Sarkyt E. Kudaibergenov [d], Vitaliy V. Khutoryanskiy [e,*]

[a] K. Zhubanov Aktobe Regional State University, 030000, Aktobe, Kazakhstan
[b] Institute of Pharmacy, Kazan State Medical University, 420126, Kazan, Russian Federation
[c] West Kazakhstan Medical University Named After M. Ospanov, 030000, Aktobe, Kazakhstan
[d] Institute of Polymer Materials and Technologies, Almaty, 050019, Kazakhstan
[e] School of Pharmacy, University of Reading, Whiteknights, RG6 6AD, Reading, United Kingdom

ARTICLE INFO

Keywords:
Films
Gellan gum
Glaucoma
Miscibility
Mucoadhesion
Ocular drug delivery
Pilocarpine hydrochloride
poly(2-oxazoline)

ABSTRACT

The study aims to develop new prolonged delivery systems of pilocarpine hydrochloride (pilocarpine·HCl) for the therapy of glaucoma. Polymer films based on gellan gum (GG) and its mixtures with poly(2-ethyl-2-oxazoline) (POZ) at different ratios were prepared by casting. The films were found to be homogeneous, transparent, and sufficiently flexible. The GG:POZ mixtures were examined using spectroscopic, thermal and microscopic methods. Additionally, the mechanical and mucoadhesive properties of GG and GG:POZ films were studied. It was found that the greater content of gellan gum in the mixture enhances the mechanical strength and mucoadhesive properties of GG:POZ films. In *vivo* experiments in rabbits were conducted to evaluate the practical application of these films loaded with pilocarpine hydrochloride. The results demonstrate the effectiveness of the polymeric films compared to traditional eye drops in terms of prolonged release of the miotic drug and extended therapeutic effect duration.

1. Introduction

The term "glaucoma" describes a group of ocular conditions with several characteristic features: firstly, it is a constant or periodic increase in intraocular pressure (IOP) above the individually tolerated levels; secondly, it is the development of specific visual field lesions and optic nerve atrophy, which can ultimately lead to blindness [1]. This disease has a profound negative effect on the psychological, social, and emotional well-being of the patients. There are two most common forms of glaucoma: open-angle glaucoma (leads to excessive fluid production) and closed-angle glaucoma (leads to rapid, painful, and irreversible loss of vision up to blindness). Unfortunately, modern ophthalmology is not yet able to completely cure a person from glaucoma, but with regular medication, intraocular pressure can be controlled and the damage to the optic nerve can be prevented. Ophthalmologists use various therapeutic agents to treat glaucoma, such as β-blockers, prostaglandin analogues, carbonic anhydrase inhibitors, sympathomimetics and miotics [2]. Drug therapy is usually prescribed in the form of antiglaucoma eye drops, which require strict adherence to the administration schedule. Patients diagnosed with glaucoma are typically required to administer eye drops throughout their life.

Pilocarpine is one of the drugs used to treat angle-closure glaucoma. It is available as eye drops of 1–2% pilocarpine hydrochloride or pilocarpine nitrate. However, due to the physiological barriers, topically administered pilocarpine drops result in a low drug bioavailability of 1–3% in the eye [3]. In this regard, there is a strong interest in developing effective drug delivery systems for glaucoma therapy [4].

Various mucoadhesive delivery systems for pilocarpine targeting eye tissues have been developed for the therapy of glaucoma. Durrani et al. [5] explored the use of Carbopol 1342 as a mucoadhesive polymer to improve the intensity and duration of the miotic response of pilocarpine nitrate incapsulated in liposomes using albino rabbits. Saettone with

* Corresponding author. Reading School of Pharmacy, University of Reading, Whiteknights, PO Box 224, RG6 6AD, Reading, United Kingdom.
** Corresponding author. Regional State University, Aktobe, 030000, Kazakhstan.
E-mail addresses: guzelab82@mail.ru (G.K. Abilova), v.khutoryanskiy@reading.ac.uk (V.V. Khutoryanskiy).

https://doi.org/10.1016/j.jddst.2024.106492
Received 28 October 2024; Received in revised form 29 November 2024; Accepted 4 December 2024
Available online 4 December 2024

co-workers [6] reported the design of cylindrical ocular inserts based on blends of poly(vinyl alcohol), glyceryl behenate and different polymers (xanthan gum, jota-carrageenan, hydroxypropyl methylcellulose, and hyaluronic acid) for formulating pilocarpine nitrate using an extrusion technique. These inserts were then coated with a mixture of Eudragit RL and RS. The miotic activity tests conducted using these inserts established prolonged drug release and improved performance in the case of the coated formulations compared to uncoated ones. Choy et al. [7] demonstrated the sustained release of pilocarpine using mucoadhesive microparticles in a rapidly dissolving tablet, while İnce et al. [8] developed a pilocarpine microemulsion with good physicochemical properties and stability. The potential of mucoadhesive poly ((2-dimethylamino)ethyl methacrylate) nanogels for sustained release of pilocarpine was also reported by Brannigan et al. [9].

Ocular films have gained significant attention as emerging drug delivery platforms, offering sustained drug release, improved bioavailability, and enhanced patient comfort [10,11]. These thin, transparent polymeric matrices, when applied directly onto the ocular surface, provide prolonged contact time, reduced systemic absorption, and minimized side effects compared to traditional eye drops. Incorporating pilocarpine, a well-established miotic agent, into ocular films presents a promising approach for optimizing glaucoma therapy. Hsiue et al. [12] has reported that polymers such as poly(2-hydroxyethylmethacrylate) can significantly improve the bioavailability and retention of pilocarpine in the ocular tissues. Wafa et al. [13] studied ocular inserts and in situ film-forming liquids, finding comparable efficacy for delivering pilocarpine. Alotaibi et al. [14] reported the development of ocular inserts (films) based on blends of hydroxypropylmethylcellulose with poly (vinyl alcohol) and loaded these with pilocarpine hydrochloride encapsulated in niosomes. They demonstrated that these inserts could ensure a sustained release of the drug over 24 h in *in vitro* experiments. These studies collectively highlight the potential of mucoadhesive films for ocular pilocarpine delivery, with the need for further research to optimize their performance.

The development of drug delivery vehicles relies on different natural and synthetic polymers, each with their own advantages and challenges [15–18]. Natural polysaccharides exhibit remarkable properties, making them widely favored and valuable for a range of biomedical applications [19]. Among them, gellan gum, a polysaccharide derived from aerobic fermentation, stands out as a promising material with excellent film-forming properties due to its malleability and high efficiency. The films based on gellan gum have found applications in formulations for wound healing, bone regeneration, and drug delivery systems. Gellan gum is already used as a component of ocular formulations for the therapy of glaucoma, for example, eye drops called Timoptol TM with timolol maleate are available commercially [20]. Previously, Agibayeva et al. [21] reported chemically modified gellan gum with enhanced mucoadhesive properties for delivery of pilocarpine hydrochloride to the eye.

Formulation of ocular films using water-soluble polymers often requires optimization of their properties to meet several requirements such as mechanical properties and integrity, swellability, and tailored mucoadhesive properties. One of the strategies to achieve these optimal film formulations is blending of different water-soluble polymers. Previously, we reported optimization of polymeric films by blending chitosan with poly(2-ethyl-2-oxazoline) as a non-ionic water-soluble polymer [22]. Although we did achieve some optimal film characteristics, this study did not involve any model drug formulation and its efficiency evaluation.

In this study we explored the preparation of ophthalmic films with pilocarpine hydrochloride by blending gellan gum with poly(2-ethyl-2-oxazoline). The physicochemical properties of these films were evaluated at different polymer ratios using thermal methods, Fourier-transform infrared spectroscopy and scanning electron microscopy. Mucoadhesive properties of these films were studied with *ex vivo* ocular tissues using a tensile test. Non-invasive in vivo experiments performed on rabbits provided valuable information about the efficiency of these formulations. As far as we are aware, this is the first investigation into the miscibility of these polymers and application of their blends in ocular drug delivery.

2. Experimental section

2.1. Materials

Gellan gum (Gelzan™ CM – Gelrite®, MW ~ 1000–2000 kDa, GG), poly(2-ethyl-2-oxazoline) (POZ, MW ~ 50 kDa, PDI 3–4) were purchased from Sigma-Aldrich (Gillingham, UK). Pilocarpine hydrochloride was purchased from Merck (Brazil).

2.2. Preparation of drug-free films

All films were prepared using the solution casting and solvent evaporation method. To prepare a 0.75 % w/v gellan gum solution, 3.75 g of pure polymer powder was dissolved in 500 mL of deionized water with continuous stirring at 60 °C for 3–4 h. Poly(2-ethyl-2-oxazoline) solutions (1.0 % w/v) were prepared by dissolving 5.0 g of polymer in 500 mL of deionized water with a pH of 6.8 and continuous stirring for 1 h. The film-forming mixtures were prepared by blending aqueous solutions of gellan gum and poly(2-ethyl-2-oxazoline) at different volume ratios. The blend films were designated as follows: the uppercase letters GG represented the gellan gum component, and the uppercase letters POZ represented the poly(2-ethyl-2-oxazoline) component in the blend. The blends were denoted by GG:POZ followed by volume ratios enclosed in parentheses, such as (100), (90:10), (80:20), (70:30), (60:40), (50:50), (40:60) and (30:70). All film-forming solutions were thoroughly mixed using magnetic stirring for 30 min at 1500 rpm. Once a homogeneous solution was achieved, it was poured into a Petri dish and left at room temperature for several days until the solvent had fully evaporated. To study the mechanical and mucoadhesive properties, films were prepared by adding 0.5 % w/v glycerol to increase their flexibility.

2.3. Preparation of pilocarpine hydrochloride – loaded films

Films loaded with two different concentrations of pilocarpine hydrochloride were prepared. For this purpose, precise amounts of pilocarpine hydrochloride, 0.084 g and 0.042 g, were dissolved in 30 mL of a prepared GG:POZ (60:40) solutions over 60 min until complete homogenization. The prepared solutions were then poured into 9 cm diameter Petri dishes and dried as previously described. The content of pilocarpine hydrochloride in each rectangular drug film with an area of 0.5 cm^2 was either 3.8 mg or 7.5 mg.

2.4. Fourier transform infrared (FTIR) spectroscopy

FTIR spectra were recorded using a Cary 660 Agilent FTIR spectrometer (Agilent Technologies, USA) with an attenuated total reflectance accessory featuring a diamond crystal.

2.5. Modulated differential scanning calorimetry (mDSC)

Modulated differential scanning calorimetry (mDSC) measurements were conducted using a Discovery DSC™ (TA Instruments, New Castle, DE, USA) with a refrigerated cooling system (RCS90). Data analysis was performed with TRIOS™ software (version 5.1.1.46572, TA Instruments, New Castle, DE, USA). All calorimetric experiments utilized Tzero aluminum pans (TA Instruments, New Castle, DE, USA), with an empty pan as the reference. Dry nitrogen was used as purge gas at a flow rate of 50 mL/min. Samples (3–5 mg) were initially cooled from room temperature to 10 °C, held at 10 °C for 5 min, then heated to 150 °C. The modulation settings included a heating rate of 2 °C/min, a modulation

period of 60 s, and an amplitude of 0.636 °C. Afterward, the samples were rapidly cooled back to 10 °C, held for 5 min, and reheated to 150 °C under identical conditions. Glass transition temperatures were determined during the second heating cycle using the reversing heat-flow signals. All measurements were conducted in triplicates.

2.6. Thermogravimetric analysis (TGA)

TGA of pure GG, pure POZ, and the GG/POZ blend samples was carried out using a Discovery TGA instrument (TA Instruments, New Castle, DE, USA). The analysis was conducted from 30 to 500 °C at 10 °C/min heating rate in a nitrogen atmosphere. The moisture content in the films was evaluated using the weight loss observed in the initial step of their TGA thermograms (up to approximately 150 °C).

2.7. Scanning electron microscopy (SEM)

SEM experiments used a FEI Quanta 3D 200i Scanning Electron Microscope instrument (FEI UK Ltd., UK). To achieve high-resolution imaging, the measurements were conducted in high-vacuum mode employing a secondary electron detector, with an applied accelerating voltage of 20 kV. Prior to imaging, the surfaces of the GG and GG:POZ films were sputter-coated with a thin layer of gold to enhance image clarity. The specimens were securely mounted on aluminum stubs using carbon adhesive tape to ensure stability during the examination process.

2.8. Mechanical analysis

The puncture strength (PS) and elongation at break (EB) values of the samples were determined using a TA.XT Plus Texture Analyser (Stable Micro Systems Ltd., UK) in a compression mode, and the tests were conducted at room temperature. Film thickness values were measured using a handheld micrometer, with 6 measurements taken at different positions for each sample, and the mean values were subsequently calculated. The average film thickness was 0.065 ± 0.002 mm.

For the testing procedure, square-shaped film samples measuring 30 × 30 mm were secured between two plates with a cylindrical hole of 10 mm diameter, resulting in a sample holder hole area of 78.54 mm^2. These samples were compressed using an upper load of a 5 mm stainless steel spherical ball probe (P/5S) at a test speed of 1.0 mm/s. The plate was stabilized using two pins to prevent any movements.

The following testing parameters were used: a pre-test speed of 2.0 mm/s, a test speed of 1.0 mm/s, a post-test speed of 10.0 mm/s, target mode set to distance with a target distance of 5 mm, an auto-trigger type, and a trigger force of 0.049 N. The film samples were punctured, and the puncture strength was then calculated using the following equation [23,24]:

$$PS = \frac{Force}{Ar_s} \quad (1)$$

where Force is the maximal force recorded during the strain.

Elongation at break (EB) is defined as the ratio of the film's extension at the rupture point to its initial length, expressed as a percentage:

$$EB = \left(\frac{\sqrt{a^2 + b^2 + r}}{a} - 1 \right) \times 100\% \quad (2)$$

where a' is the initial length of the sample that is not punctured by the probe; b is the penetration depth/vertical displacement by the probe; r is the radius of the probe; and a is the radius of the film in the sample holder opening. All experiments were performed 3 times, and the average values along with standard deviations were computed and statistically analyzed.

2.9. Ex vivo mucoadhesion studies

The investigation into the mucoadhesive characteristics of the films on the mucosal surface of sheep's eyes utilized a tensile method, employing a Texture Analyser XT Plus (Stable Micro Systems Ltd., UK) with a cylindrical aluminum probe P/10, measuring 10 mm in diameter. To conduct the experiments, each film was cut into 10 mm discs and subsequently affixed to the probe using a double-sided adhesive tape.

Sheep eyes were procured from Altyn-Orda Abattoirs (Almaty, Kazakhstan) following animal slaughter. Each ocular mucosal tissue specimen was firmly attached to the mucoadhesion rig and moistened with artificial tear fluid (ATF) prior to each test. ATF was prepared in accordance with our previous report [22] and comprised the following components: 3.35 g NaCl, 1 g $NaHCO_3$, and 0.0305 g $CaCl_2$, dissolved in 500 mL of deionized water.

During the adhesion experiments, each film sample, secured to the cylindrical probe, was gently pressed onto the moist conjunctiva of a sheep's eye, maintaining contact for 30 s to ensure full attachment. Subsequently the probe was retracted until full detachment from the biological substrate was achieved. All adhesion experiments were performed using the following settings: pre-speed test 0.5 mm/sec; test-speed 0.5 mm/sec; post-test speed 10.0 mm/sec; applied force 100 g; return distance 10 mm; contact time 30 s; trigger type auto; trigger force 0.049 N. Each experiment was repeated five times using different sheep eyes.

Data derived from these experiments were employed to evaluate the film's mucoadhesive strength. This assessment encompassed determining the maximum force required for detachment (F_{adh}) and computing the total work of adhesion, represented as the area under the force/distance curve (W_{adh}). Each film sample underwent these measurements five times, ensuring a thorough and dependable analysis of their adhesive properties when in contact with the sheep's eye conjunctiva.

2.10. In vivo experiments

In vivo experiments with drug-loaded films were performed using chinchilla rabbits (2350–2920 g, both males and females) according to a previously described protocol [21]. These experiments were approved by Marat Ospanov West Kazakhstan Medical University (Kazakhstan, Aktobe) ethics committee (approval No. 3 from March 28, 2023) and were performed in accordance with the ARVO Statement for the Use of Animals in Ophthalmic and Visual Research. All rabbits were kept in standard cages and had unrestricted access to food and water. Before the start of experiments, chinchilla rabbits were randomly assigned into 4 groups (n = 3). All rabbits were acclimatized to laboratory testing conditions for 30 min before the study. Each rabbit was carefully swaddled in cotton cloth during the experiment to prevent them from touching their eyes and displacing the polymer film. However, their eye and eyelid movements were not restricted. The pupil diameters were evaluated using a wooden ruler at a fixed distance from the rabbit's eye. The dosage form—either eye drops containing 1 % pilocarpine hydrochloride or polymer films with varying concentrations of pilocarpine hydrochloride, - was applied to the lower conjunctiva of the rabbit's left eye. A 0.9 % NaCl solution was instilled into the right eye as a control, and the pupil diameter of both eyes was measured. The diameters of the left and right pupils were measured alternately three times, and the average value was calculated. The above procedure was repeated using films measuring 3 × 5 mm containing 3.8 and 7.5 mg of pilocarpine hydrochloride and drug-free films. The pupil diameters of the right and left eyes were measured at the following time intervals: 0, 10, 20, 30, 60, 90, 120, 150, 180, 210, and 240 min. At these time intervals, digital images were acquired using a web-camera and then processed using ImageJ software to calculate the difference in pupil diameter between the right (D_{right}, mm) and left (D_{left}, mm) eyes:

$$\Delta = D_{right} - D_{left} \quad (3)$$

To evaluate the pharmacological response of the different formulations, the areas under the curve for the decrease in pupil diameter (Δpupil diameter, after baseline correction) over a 240-min period (AUC_{0-240}) were determined using the trapezoidal rule.

2.11. Statistical analysis

The results of all experiments are presented as mean ± standard deviation from at least 3 independent experiments. For mechanical studies at least three and for mucoadhesion studies at least five different specimens were used for each measurement. The data, represented as mean values ± standard deviations, were evaluated for significance with a two-tailed Student's t-test and a one-way ANOVA followed by a Bonferroni post hoc test, conducted with GraphPad Prism software (version 7.0). A p-value <0.05 was considered statistically significant.

3. Results and discussion

3.1. Preparation and characterisation of films

The film casting method was chosen for this study because of its cost-effectiveness and ease of preparation at the laboratory scale. All the films prepared with the GG:POZ combination displayed homogeneity, though with slight brittleness. They appeared transparent, devoid of insoluble particles, and could be easily removed from Petri dishes. The addition of glycerol as a plasticizer resulted in softer and more flexible films compared to those without this compound.

During preliminary trial by varying the amount of glycerol (between 0.25 and 1.25 % w/v) different formulations were prepared. The composition GG:POZ (60:40), which exhibited the desired characteristics of texture and uniform thickness, was chosen for the preparation of ocular films containing pilocarpine hydrochloride.

3.2. Fourier transform infrared spectroscopy (FTIR)

FTIR spectral analysis of pure gellan gum, pure poly(2-ethyl-2-oxazoline) (POZ), and their drug-free blends offers valuable insights into the molecular interactions between the polymers (Fig. 1). The FTIR spectrum of gellan gum contains several characteristic absorption bands associated with carboxyl and hydroxyl groups. The absorption band centered at 3300 cm^{-1} shows the presence of free or associated hydroxyl groups (O-H). The absorption band in the 3000-2800 cm^{-1} range is associated with stretching vibrations of the valence bonds of C-H in alkyl groups [25]. Carbonyl groups (C=O) within the gellan gum are present in relatively low quantities, resulting in a low absorption intensity at the vibrational frequency of 1609 cm^{-1} in the spectrum of pure gellan gum. The absorption bands at 1452 and 1407 cm^{-1} are indicative of deformative vibrations of CH_3 and CH_2 groups present in the side chains of gellan gum [25].

The absorption bands at 1230 and 1034 cm^{-1} characterize valence vibrations of C-O and C-C bonds in the glycosidic linkages of the gellan gum, respectively [26].

The spectrum of the POZ film reveals the broad absorption band at 3372 cm^{-1}, indicating the presence of bound water that has not been completely removed from the sample. The absorption bands at 2975 cm^{-1}, 2940 cm^{-1}, and 2884 cm^{-1} correspond to the valence vibrations of the $-CH_3$, $-CH_2$, and -CH groups, respectively. The absorption bands at 1626 cm^{-1}, 1424 cm^{-1}, and 1374 cm^{-1} are associated with the valence vibrations of -C=O (amide I) and the deformative vibrations of $-CH_3$ and -CH groups [27]. The interactions between gellan gum and poly (2-ethyl-2-oxazoline) can be inferred from the shift in the positions of the peaks of their respective functional groups in the FTIR spectra. The absorption band centered at 3600–3000 cm^{-1}, attributed to the stretching of OH exhibited significant changes likely due to intermolecular hydrogen bonds. In comparison to the pure POZ film, the absorption band at 3372 cm^{-1} shifted to lower wavenumbers in GG/POZ films. This shift was likely caused by hydrogen bonding due to the additional OH groups present in GG. The band observed at 3355 cm^{-1} in the GG:POZ (30:70) film shifted to 3340 cm^{-1} in the GG:POZ (90:10) films, suggesting an increase in intermolecular hydrogen bonding between GG and POZ.

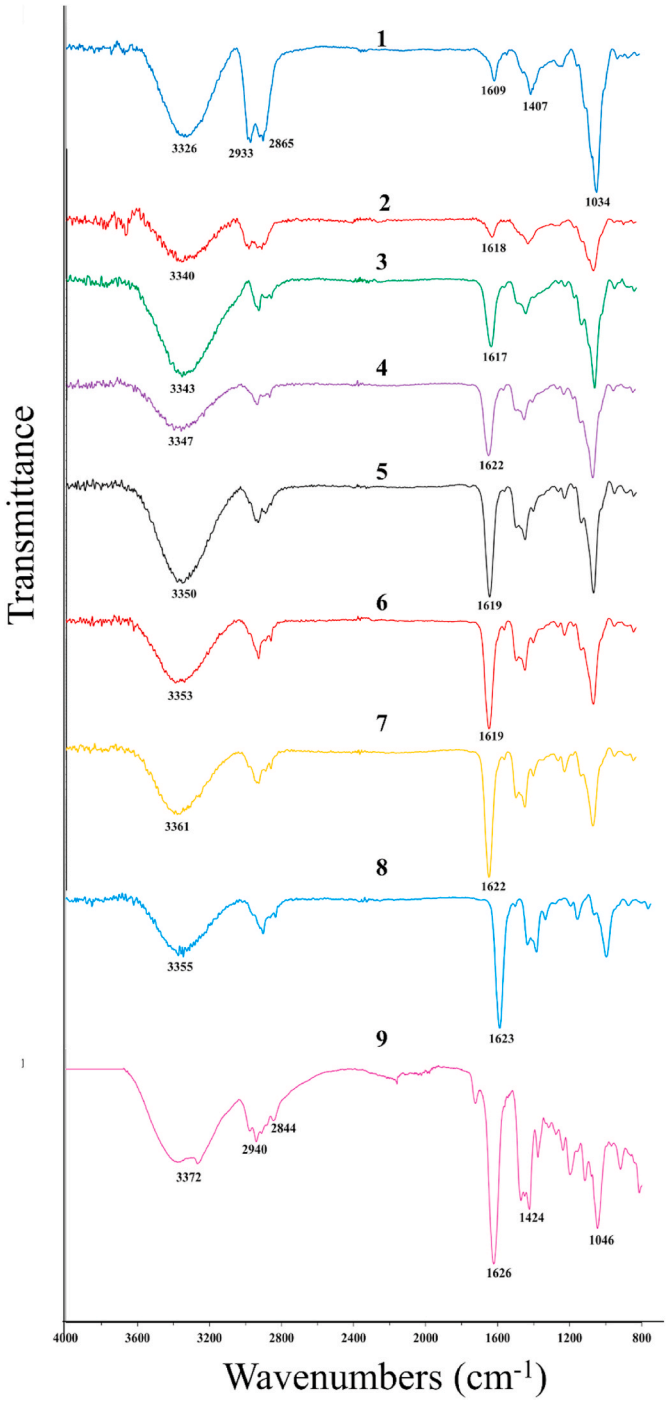

Fig. 1. FTIR spectra of pure gellan gum (1), pure POZ (9) and its blends. Content of POZ in the blends: 10 (2), 20 (3), 30 (4), 40 (5), 50 (6), 60 (7) and 70 % (8).

The band at 1623 cm^{-1} was attributed to carbonyl stretching vibrations and the shift in the carbonyl band implied the presence of hydrogen bonding between GG and POZ within the films. This band, initially observed at 1623 cm^{-1} in the GG:POZ (30:70) film shifted to

1618 cm^{-1} in the GG:POZ (90:10) sample, indicating a possible increase in the contribution of intermolecular hydrogen bonding between the polymers forming the blend.

3.3. Differential scanning calorimetry

It is widely recognized that the compatibility of polymers necessitates blending at a molecular level, thereby averting phase separation within the composite. Miscible polymer blends should display a single glass transition temperature (Tg), observed between the Tg values characteristic of the individual components. Conversely, in instances of incompatible components, both Tg values will be present and will remain relatively unchanged.

The miscibility analysis of GG:POZ polymer blends was conducted employing differential scanning calorimetry (DSC), a technique widely recognized for its precision in characterizing thermal transitions within materials. DSC thermograms of pure gellan gum, pure POZ, and their blends are shown in Fig. 2. The glass transition temperature (Tg) of pure POZ is observed at 56 °C, which is in agreement with the literature data [28]. Notably, in the case of pure gellan gum, a discernible Tg peak was not observed in the thermogram.

This can be explained by a semicrystalline nature of this polymer [29]. The crystalline regions present in the polymer may limit the mobility of the amorphous chains, making the Tg difficult to detect against other processes. Additionally, in polymers with high crystallinity, the Tg can be masked by broader thermal transitions like melting or degradation. According to the literature, the Tg of gellan is 40–60 °C [30,31]. The difficulties of detecting the glass transition temperature using DSC were also observed by us previously for other polysaccharides such as chitosan [22].

In GG:POZ blends, a single glass transition temperature (Tg) was observed at approximately 60 °C, slightly higher than the value for pure POZ, though the difference was minimal.

The detection of a single Tg on the thermograms of these blends suggests the presence of intermolecular interactions between the polymers, resulting in a fully miscible blend structure where macromolecules of both polymers are mixed at the molecular level. Furthermore, the crystalline regions of gellan gum may contribute to stabilization of the blend, preventing significant shifts in the Tg when POZ is added.

Notably, in the blends with lower POZ content, specifically at (90:10) and (80:20) ratios, a distinct glass transition temperature was not clearly identified on the thermograms. This could be attributed to the dominance of the gellan gum in these blends, which restricts the mobility of the amorphous regions, thereby hindering the detection of the glass transition.

3.4. Thermogravimetric analysis

A thermogravimetric analysis was conducted for GG:POZ films with various compositions to assess their thermal stability and mass loss behavior. This analysis aimed to further understand their compatibility, as deviations in degradation temperatures provide additional insights into the miscibility of polymers in the blends. The TGA curves for the films are shown in Fig. 3. Pure GG films exhibited two degradation stages in the thermogram. Initially, a minor weight loss occurred between 60 °C and 150 °C, attributed to the evaporation of water, whose molecules are physically associated with the polymer matrix, constituting approximately 11 % of the sample. The second stage, observed between 230 °C and 250 °C, is likely due to the degradation of GG, leading to chain destruction via dehydration, deamination, and ring-opening reactions [32].

In contrast, pure POZ films demonstrated greater thermal stability compared to 100 % GG. The initial weight loss, starting above 50 °C, involved the removal of physically-bound water, accounting for approximately 3.2 % of the total weight. The second stage of decomposition commenced above 383 °C [28], with the maximum degradation rate observed at 410 °C, resulting in 96 % weight loss at 420 °C. These findings are consistent with our previous studies, which reported also a single decomposition stage of POZ at approximately 400 °C [22,33]. The thermal behavior of GG:POZ blends showed a three-step decomposition profiles: in the first stage, spanning from 50 °C to 150 °C, there is a loss of physically bound water; in the second stage, occurring between 225 °C and 262 °C, the degradation of gellan gum takes place; the third stage, spanning from 345 °C to 395 °C, showing the degradation of poly (2-ethyl-2-oxazoline). During the second degradation stage, the GG/POZ films with ratios of (90:10), (80:20), and (70:30) demonstrated significant weight loss of approximately 43 %, 37 %, and 33 %, respectively. In contrast, as the POZ content in the mixture increases, the formulations such as GG:POZ (60:40), GG:POZ (50:50), GG:POZ (40:60), and GG:POZ (30:70) exhibited comparatively lower weight loss rates of about 28 %, 25 %, 17 %, and 15 %, respectively. However, in the third stage, an inverse relationship was observed. Formulations of the films with the ratios of (90:10), (80:20), and (70:30) displayed weight losses of 16 %, 24 %, and 35 %, respectively. Meanwhile, GG:POZ (60:40), GG:POZ

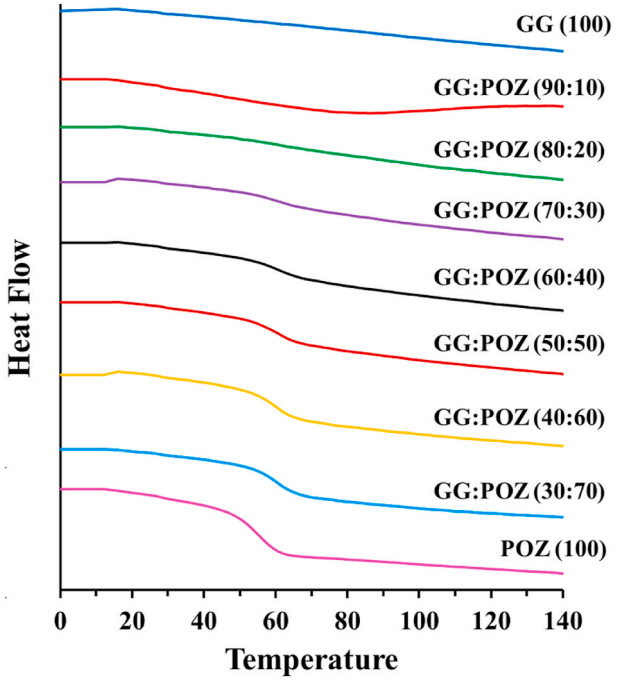

Fig. 2. DSC thermograms of pure GG, pure POZ and GG/POZ blends prepared at various polymer ratios.

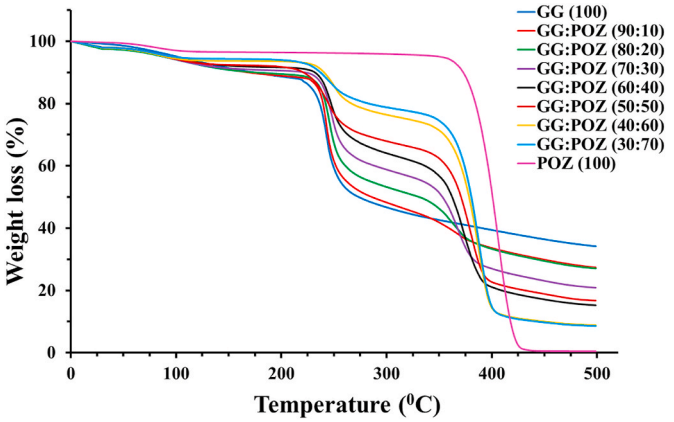

Fig. 3. TGA curves of pure GG, pure POZ and GG/POZ blends at various polymer ratios.

(50:50), GG:POZ (40:60), and GG:POZ (30:70) samples lost about 46 %, 49 %, 65 %, and 68 % of their weight, respectively. It is important to note that the temperatures at which the degradation rates for stages 2 and 3 peaked exhibited a strong correlation with the blend composition. The results indicated that a higher POZ content in the blend corresponded to a lower rate of weight loss. Thus, the presence of POZ in the blend enhances the thermal stability of GG; as the content of POZ increases, the thermal stability of the GG:POZ polymer blend also improves, which is likely related to the formation of weak hydrogen bonds between the polymers.

3.5. Scanning electron microscopy (SEM)

SEM is a very common technique to probe the compatibility between the polymers in the blends. If two polymers are miscible, they typically form uniform blends, which is often observed in SEM images [34–36]. On the contrary, if two polymers are fully immiscible (incompatible), the blend morphology typically exhibits phase separation.

The cross-sectional morphology and surface microstructure of the polymer films were examined using scanning electron microscopy (Fig. 4).

The SEM analysis revealed that the GG:POZ films, particularly at low POZ concentrations, have a smooth and homogeneous surface. This homogeneity is likely due to the interactions and excellent compatibility between GG and POZ at these lower ratios. However, with increasing POZ content, slight changes in the surface morphology were observed. Specifically, the surfaces of the GG:POZ (70:30), GG:POZ (50:50), and GG:POZ (30:70) films demonstrated a relatively smooth texture with minimal surface irregularities, suggesting some heterogeneity in the POZ distribution within the GG matrix. Further analysis of the cross sections provided additional insight into the internal structure of the films. The pure GG sample exhibited a dense and layered structure, consistent with the surface morphology observed. In contrast, the GG:POZ (30:70) composition film displayed significant changes in the internal morphology, showing a more homogeneous and less layered internal structure. Moreover, the absence of visible defects such as pores, cracks, or bubbles indicates that the films maintained a certain degree of structural integrity, despite an increase in surface heterogeneity.

3.6. Mechanical analysis

To study the mechanical characteristics of the films, a tensile test was conducted. This is a standard method for assessing the mechanical characteristics of pharmaceutical film formulations, including ocular films. Fig. 5 presents the data on puncture strength and elongation at break for the films, with the values expressed as the mean of three independent measurements. For the film composed of pure gellan gum, the puncture strength was 1.17 ± 0.18 N/mm^2, while the elongation at the break point was 30.29 ± 6.57 %, indicating good elastic properties of this material. As the proportion of POZ in the blend increased, a consistent decline in puncture strength was observed, with the GG:POZ (30:70) film exhibiting a minimum value of 0.37 ± 0.01 N/mm^2 and an elongation at break of 21.69 ± 0.19 %.

These findings suggest that higher POZ content diminishes the resistance of the films to mechanical damage, such as punctures, and also reduces their elasticity, rendering them more brittle. Both graphs depict a nearly linear decrease in mechanical properties as the POZ content increases. This trend is likely attributed to the role of gellan gum in formation of a rigid matrix that imparts better mechanical strength. A reduction in gellan gum content in the films weakens their overall structure, as the matrix becomes less dense and less capable of withstanding mechanical stresses. This is likely due to a reduction in hydrogen bonding between gellan gum macromolecules (GG-GG) and the formation of hydrogen bonds between gellan gum and POZ (GG-POZ). The analysis confirmed that the observed decrease in the puncture strength with increasing POZ content is statistically significant, with specific differences highlighted between GG(100) and GG:POZ (50:50), GG:POZ (40:60), and GG:POZ (30:70) films ($p < 0.05$). However, the elongation at break values did not show statistically significant differences between the groups, indicating that while puncture strength is greatly affected by POZ content, the elasticity of the films remains relatively consistent across different formulations.

3.7. Mucoadhesive properties

The mucoadhesive properties of the films facilitate their better retention on mucosal surfaces. The films with strong mucoadhesive characteristics are usually capable of adhering to the mucosal surface for extended periods, thereby facilitating higher localized concentrations of the drug at the site of application. In this work, the mucoadhesive

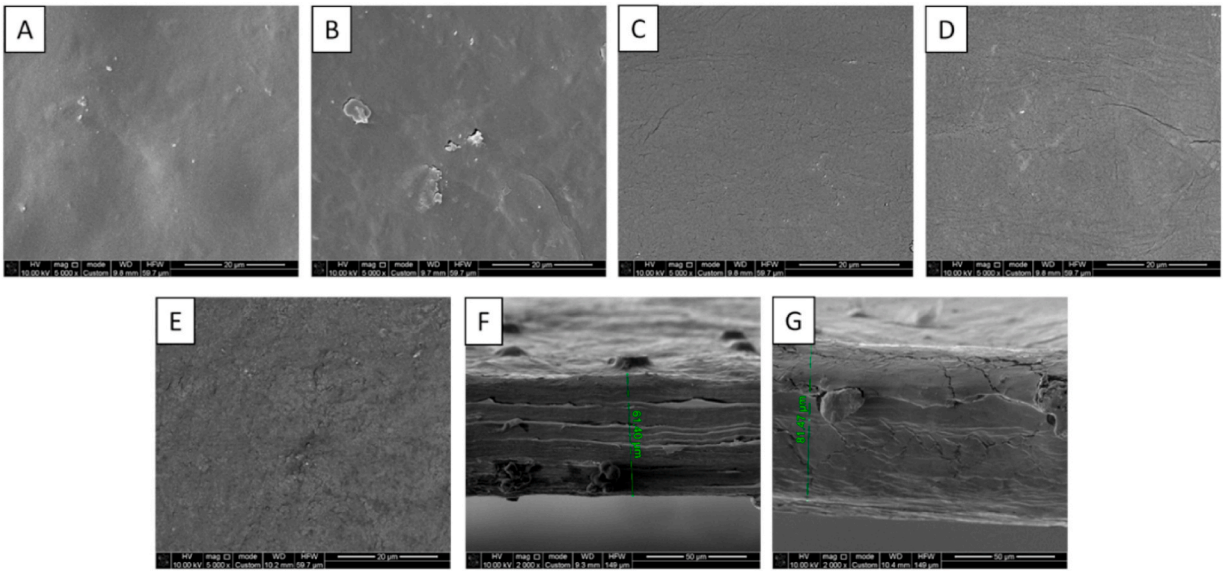

Fig. 4. SEM images of (A) pure GG and its blends with POZ (B, C, D, E) surface and cross-sections (F) pure GG and (G) GG:POZ blends. Content of POZ in the blends: 10 (B), 30 (C), 50 (D) and 70 % (E,G). Scale bars are 20 μm.

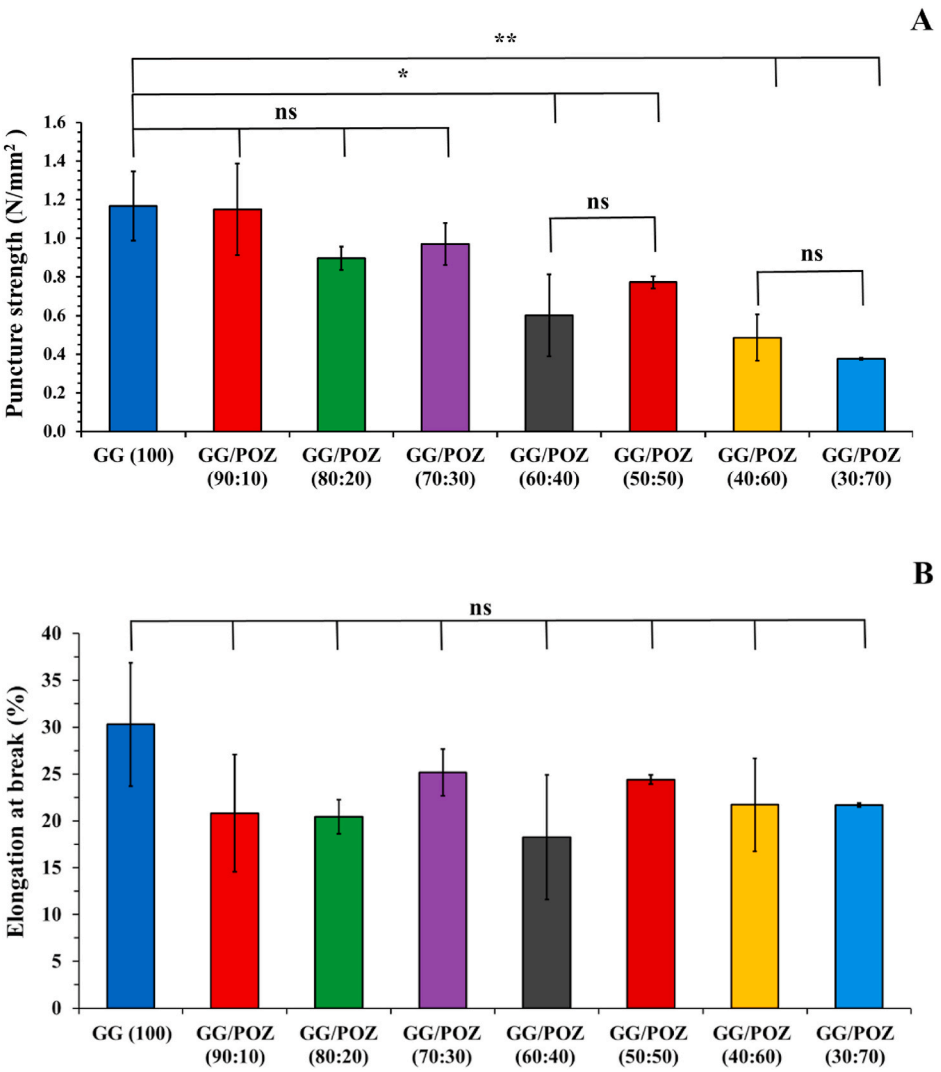

Fig. 5. Mechanical analysis of GG and GG:POZ blends: puncture strength (A) and elongation at break (B). Data are expressed as mean ± standard deviation (n = 3). Statistically significant differences are given as: ** – $p < 0.01$; * – $p < 0.05$; ns – no significance.

properties of the films were evaluated using a tensile test, employing a TA.XTPlus Texture Analyzer. This test is widely used for assessing the mucoadhesive properties of different pharmaceutical formulations, including films. Sheep conjunctiva was used as a model mucosal membrane for evaluating mucoadhesive properties. The maximum detachment force (F_{adh}) and the total adhesion work (W_{adh}) were determined for the detachment of drug-free GG and GG:POZ films from the conjunctiva of freshly excised sheep eyes (Fig. 6).

The results revealed that pure GG films (GG (100)) exhibited the highest mucoadhesive force (~0.59 ± 0.12 N) and the total work of adhesion (~0.22 ± 0.03 N·sec), confirming the strong mucoadhesive capacity of this material on the ocular mucosa. This is likely attributed to ionic nature of GG. Ionic polymers are known for their superior mucoadhesive properties compared to the non-ionic ones [37]. A significant decrease in both F_{adh} and W_{adh} was observed as the POZ content in the films increased. This reduction was particularly prominent in the GG:POZ (60:40), GG:POZ (50:50), and GG:POZ (40:60) formulations, as confirmed by statistical analysis ($p < 0.01$). These results are consistent with our previous research [22], where a similar reduction in mucoadhesive properties was observed with increasing POZ content in the blends with chitosan. Notably, POZ exhibits weak mucoadhesive properties due to its non-ionic nature, which significantly diminishes the films' ability to adhere to mucosal membranes. The formulations with lower POZ content GG:POZ (90:10) and GG:POZ (80:20) did not show significant differences compared to pure GG.

3.8. *In vivo experiments*

To evaluate the ability of GG:POZ films to deliver drugs to the eye in vivo, a formulation composed of GG:POZ (60:40) blend was prepared with inclusion of two different concentrations of pilocarpine hydrochloride. This in vivo study was conducted using rabbits to assess the efficacy of pilocarpine hydrochloride – loaded mucoadhesive films and traditional eye drops. The use of pilocarpine hydrochloride in these formulations allows non-invasive evaluation of their efficiency in vivo due to the ability of this drug to induce pupil constriction (miosis).

Previous in vivo studies have demonstrated that pilocarpine formulations incorporating gellan and its methacrylate derivatives enhance the drug's pharmacological efficacy, particularly in formulations with low-degree (~6 %) of GG methacrylation [21]. In the present study, either mucoadhesive films or eye drops were carefully administered onto rabbits lower eyelid conjunctiva of their left eye and right eye served as a control. Changes in pupil diameter were monitored by periodically capturing images with a ruler as a size reference. Fig. 7 illustrates the pupillary response in rabbits before and after administration of pilocarpine in both forms. Visual analysis revealed that both

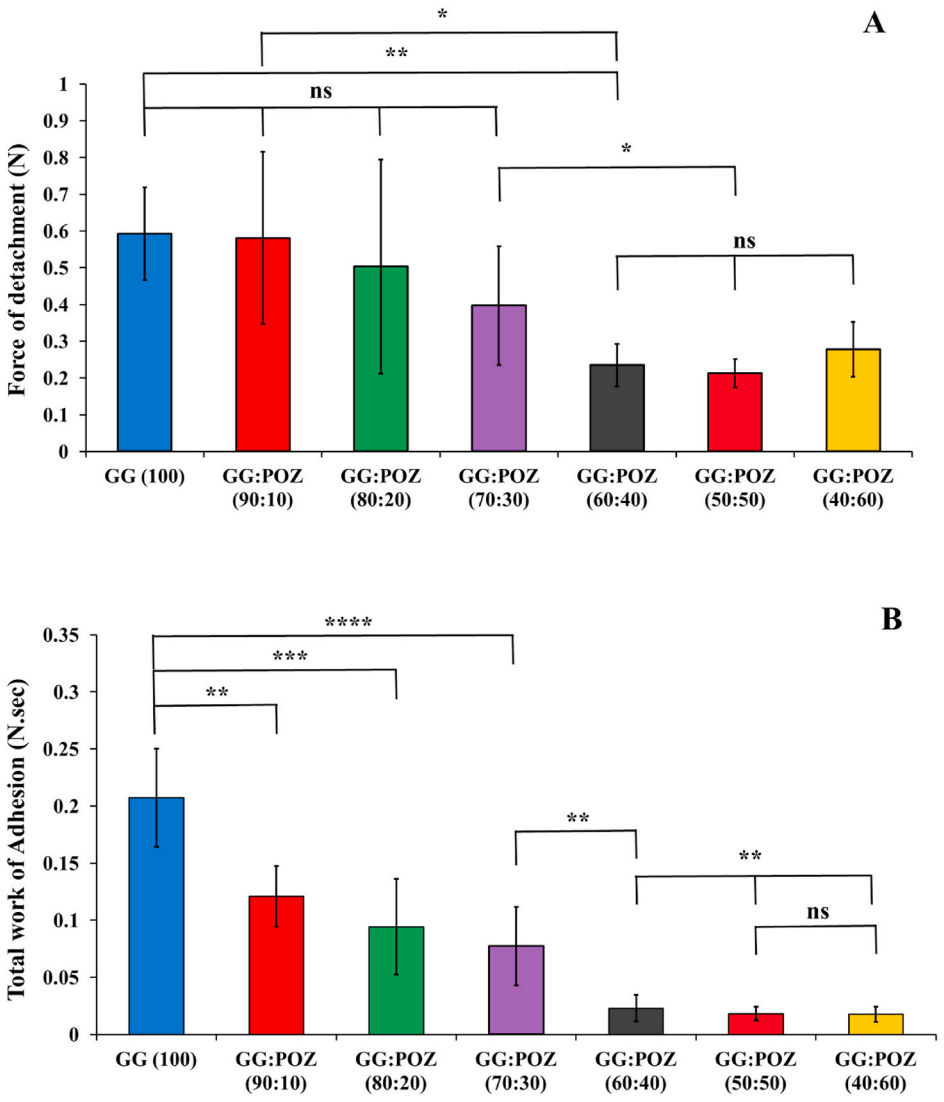

Fig. 6. Detachment force F_{adh} (A) and total work of adhesion W_{adh} (B) values for the detachment of GG and GG:POZ blend films from the conjunctiva of sheep eyes. Data are expressed as mean ± standard deviation (n = 5). Statistically significant differences are given as: **—p < 0.01; ***—p < 0.001; ****—p < 0.0001; ns—no significance.

delivery methods – eye drops and pilocarpine-loaded films – elicited a marked pupil constriction.

The results of these observations were analyzed using image analysis and are presented in Fig. 8.

It is seen that in both types of pilocarpine·HCl dosage forms (drops and films) the maximal reduction in pupil diameter is achieved in approximately 25–30 min post administration. The comparison between the curves recorded for the left eye with administered formulation and the right eye used as a control provides an opportunity to evaluate the extent of the pharmacological effect. A control experiment, where drug-free film was administered, showed no difference with the data recorded for the right eye.

Fig. 9 presents the values of Δpupil between the left and the right eyes as a function of time post administration. The polymer films induced a more prolonged and intense miosis than the eye drops. After achieving the maximal pupil constriction within the first 25–30 min post-administration, the pupil diameter values gradually returned to the baseline within 3.5 h. Notably, the difference in the duration of the effect between the formulations became apparent during this recovery phase. The constriction effect of eye drops was more short-lived, beginning to diminish within 60–90 min. In contrast, pilocarpine films produced a more sustained and consistent effect, lasting up to 240 min.

These findings are further corroborated using additional analysis by calculating the area under the curve ($AUC_{10\text{-}240}$) values (Fig. 10), which revealed statistically significant greater values for films containing 7.5 mg pilocarpine·HCl ($AUC_{10\text{-}240} = 494.54 \pm 60.17$ a.u.) compared to eye drops ($AUC_{10\text{-}240} = 163.64 \pm 59.33$ a.u.) and films containing 3.8 mg pilocarpine·HCl ($AUC_{10\text{-}240} = 377.81 \pm 207.60$ a.u.). The control group, which received polymer films without pilocarpine·HCl, exhibited minimal changes in pupil diameter ($AUC_{10\text{-}240} = 18.85 \pm 10.98$ a.u.), confirming that the observed miosis was attributable to the active pharmaceutical ingredient rather than the polymer matrix itself.

Importantly, pilocarpine·HCl films did not cause any adverse effects such as excessive tear production, tissue redness, or inflammation, suggesting good safety and tolerability for ocular application. Despite the straightforward nature of the measurements, external factors such as lighting conditions may have impacted the results. Rabbit pupils are highly sensitive to environmental light changes, which could explain some of the observed fluctuations and error margins in the graphs. Nonetheless, these variations did not alter the overall conclusion, which clearly demonstrated the superiority of polymer film formulations over eye drops. In summary, polymer films offer a more effective and sustained method of pilocarpine·HCl delivery, ensuring prolonged action and excellent safety in ocular applications.

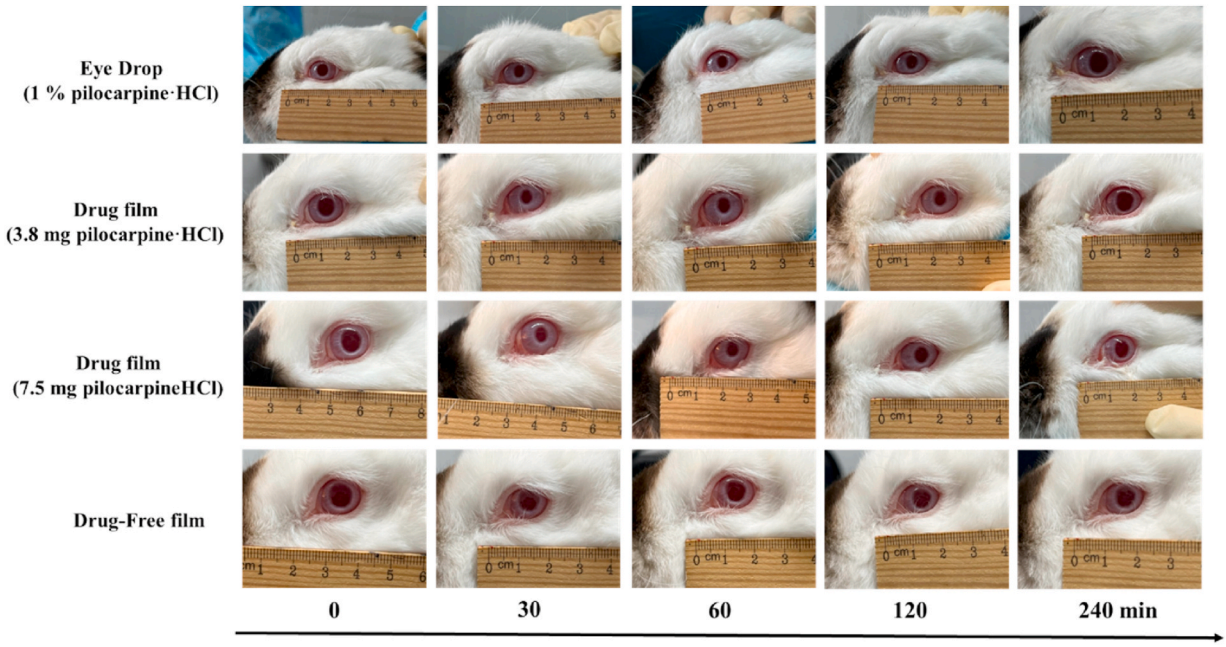

Fig. 7. Representative images of pupillary response in the left eye of rabbits in the following test groups: drug-containing eye drops, drug-containing films and drug-free film.

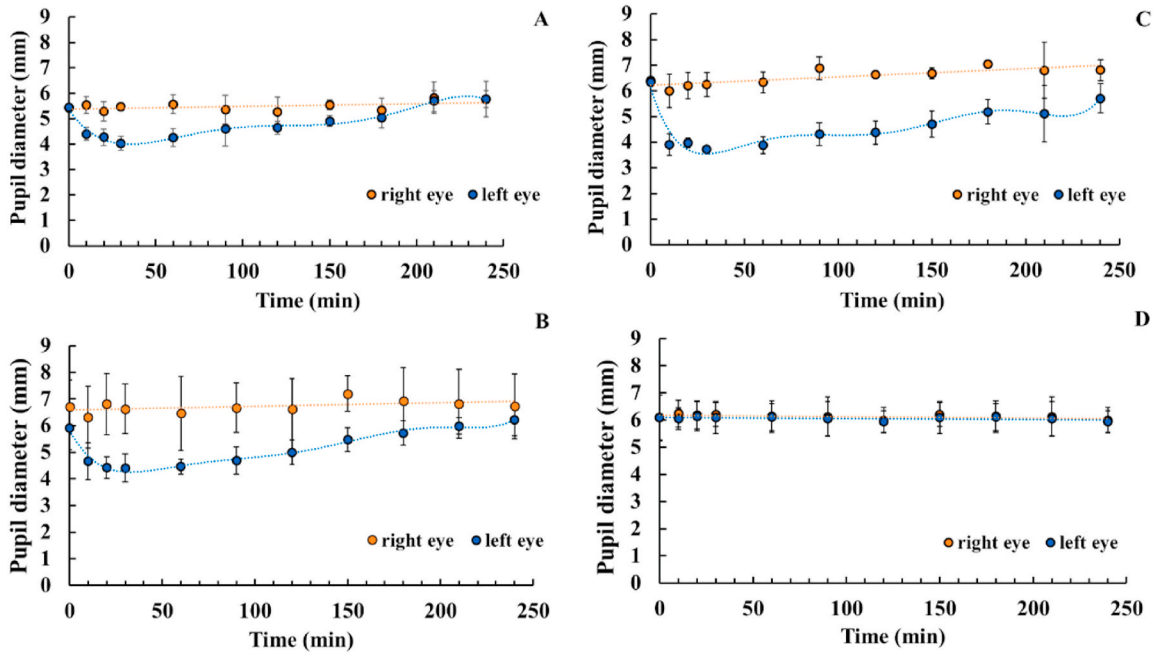

Fig. 8. Pupil diameter reduction over time for (A) 1 % pilocarpine·HCl eye drops, (B) 3.8 mg pilocarpine·HCl-containing film, (C) 7.5 mg pilocarpine·HCl-containing film and (D) frug-free film. All measurements were performed in triplicate using different rabbits (n = 3).

4. Conclusions

This study successfully developed and thoroughly characterized polymer films composed of gellan gum and poly(2-ethyl-2-oxazoline) for the ocular delivery of pilocarpine hydrochloride. The films demonstrated excellent miscibility, mechanical, thermal and textural properties, as confirmed by FTIR, DSC, and TGA analyses. These studies confirmed the compatibility of the polymer components and revealed the presence of intermolecular interactions that contributed to the structural stability of the films. The films exhibited sufficient mechanical strength and elasticity, making them suitable for ocular applications, while good mucoadhesive properties of gellan gum facilitated their prolonged retention on the ocular surface, ensuring sustained drug release.

In vivo experiments using rabbits further confirmed the efficacy of these polymer films as a pilocarpine hydrochloride delivery system. The films provided a more prolonged and intense miotic effect compared to conventional eye drops. The pharmacological effect was sustained for up to 240 min, as evidenced by the area under the curve ($AUC_{10\text{-}240}$) analysis. Additionally, the polymer films demonstrated excellent safety and tolerability, with no observed side effects such as excessive tear production, tissue redness, or inflammation of the eyes.

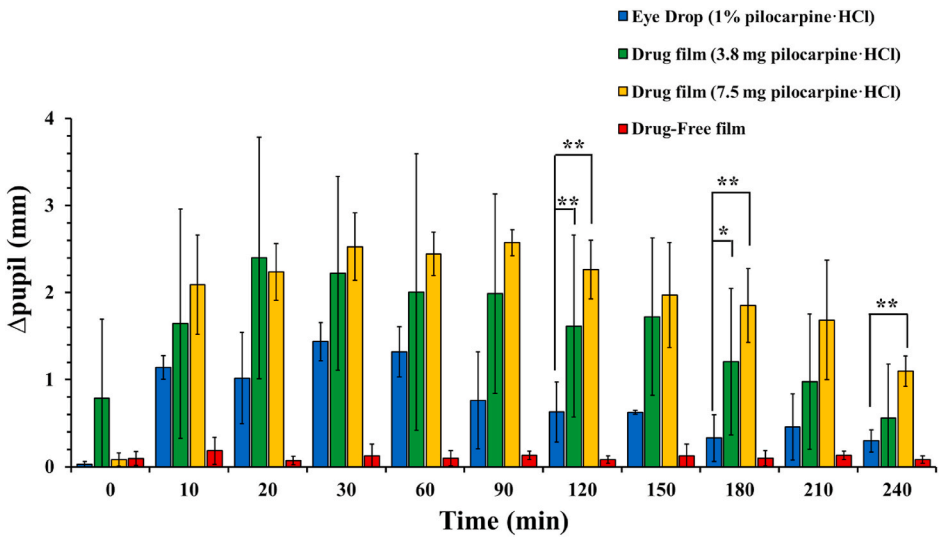

Fig. 9. Δpupil values measured in rabbits from 0 to 240 min following the administration of various pilocarpine·HCl formulations. The data are presented as the mean ± standard deviation (n = 3). Statistically significant differences are indicated as follows: *p < 0.05; **p < 0.01.

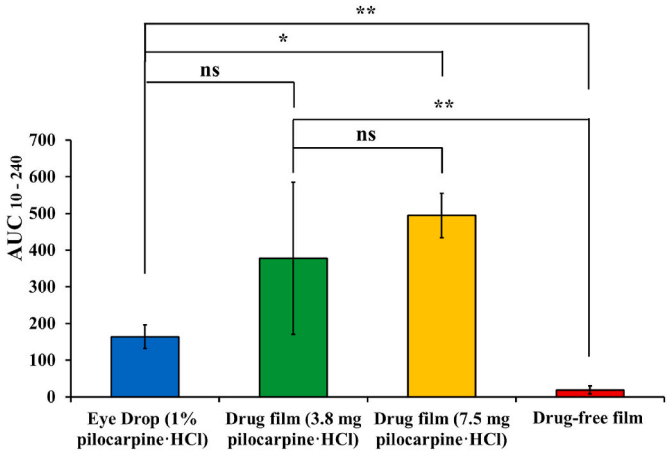

Fig. 10. Values of the area under the Δpupil versus time profiles in 240 min (AUC_{10-240}) recorded for different films. Data are expressed as mean ± standard deviation (n = 3). The data are presented as the mean ± standard deviation (n = 3). Statistically significant differences are indicated as follows: *—p < 0.05; **—p < 0.01; ns—no significance.

In conclusion, polymer films based on gellan gum and poly(2-ethyl-2-oxazoline) blends represent a promising platform for the sustained ocular delivery of pilocarpine hydrochloride in glaucoma treatment. They offer enhanced bioavailability, improved retention on the ocular surface, and a high degree of safety, making them a viable and effective alternative to traditional eye drop formulations.

CRediT authorship contribution statement

Guzel K. Abilova: Writing – original draft, Supervision, Methodology, Investigation, Formal analysis, Data curation. **Shamil F. Nasibullin:** Investigation. **Kuanysh Ilyassov:** Investigation. **Aslan N. Adilov:** Investigation. **Marzhan K. Akhmetova:** Resources, Methodology, Investigation, Formal analysis. **Rouslan I. Moustafine:** Supervision, Resources. **Yesset T. Muratov:** Resources, Investigation. **Sarkyt E. Kudaibergenov:** Supervision, Resources, Funding acquisition. **Vitaliy V. Khutoryanskiy:** Writing – review & editing, Supervision, Project administration, Funding acquisition, Conceptualization.

Declaration of generative AI and AI-assisted technologies in the writing process

During the preparation of this work the authors used ChatGPT in order to refine the language of the manuscript. After using this tool/service, the authors reviewed and edited the content as needed and take full responsibility for the content of the publication.

Declaration of competing interest

The authors declare the following financial interests/personal relationships which may be considered as potential competing interests: Guzel K. Abilova reports financial support was provided by Science Committee of the Ministry of Science and Higher Education of the Republic of Kazakhstan. Vitaliy V. Khutoryanskiy and Sarkyt E. Kudaibergenov report financial support was provided by European Union. Vitaliy Khutoryanskiy reports financial support was provided by The Royal Society. The other authors declare that they have no known competing financial interests or personal relationships that could have appeared to influence the work reported in this paper.

Acknowledgements

The authors would like to thank Zhandos Tolepov (Al-Farabi Kazakh National University, Almaty, Kazakhstan) for assistance in scanning electron microscopy experiments and Daulet Kaldybekov (Al-Farabi Kazakh National University, Almaty, Kazakhstan) for FTIR spectroscopy experiments and assistance in statistical analysis. G.K.A. would like to thank the Science Committee of the Ministry of Science and Higher Education of the Republic of Kazakhstan for the research grant for young scientists « Zhas Galym » No. AP15473201. We would also like to thank Svetlana Sakhanova (Scientific and Practical Centre of M. Ospanov West Kazakhstan Medical University) for providing an opportunity to work in the vivarium for in vivo experiments. V.V.K. and S.E.K. are grateful for the funding provided by the European Union's Horizon 2020-MSCA-RISE-2018/823883: Soft Biocompatible Polymeric NANOstructures: A Toolbox for Novel Generation of Nano Pharmaceuticals in Ophthalmology (NanoPol). V.V.K. also extends his gratitude to the Royal Society for the support provided through his industry fellowship (IF\R2 \222031).

Data availability

Data will be made available on request.

References

[1] D.A. Lee, E.J. Higginbotham, Glaucoma and its treatment: a review, Am. J. Heal. Pharm. 62 (2005) 691–699, https://doi.org/10.1093/ajhp/62.7.691.

[2] R.V. Moiseev, P.W.J. Morrison, F. Steele, V.V. Khutoryanskiy, Penetration enhancers in ocular drug delivery, Pharmaceutics 11 (2019) 321, https://doi.org/10.3390/pharmaceutics11070321.

[3] S.N.S. Anumolu, Y. Singh, D. Gao, S. Stein, P.J. Sinko, Design and evaluation of novel fast forming pilocarpine-loaded ocular hydrogels for sustained pharmacological response, J. Contr. Release 137 (2009) 152–159, https://doi.org/10.1016/j.jconrel.2009.03.016.

[4] Z.K. Al-Qaysi, I.G. Beadham, S.L. Schwikkard, J.C. Bear, A.A. Al-Kinani, R.G. Alany, Sustained release ocular drug delivery systems for glaucoma therapy, Expert Opin. Drug Deliv. 20 (2023) 905–919, https://doi.org/10.1080/17425247.2023.2219053.

[5] A.M. Durrani, N.M. Davies, M. Thomas, I.W. Kellaway, Pilocarpine bioavailability from a mucoadhesive liposomal ophthalmic drug delivery system, Int. J. Pharm. 88 (1992) 409–415, https://doi.org/10.1016/0378-5173(92)90340-8.

[6] M.F. Saettone, M.T. Torracca, A. Pagano, B. Giannaccini, L. Rodriguez, M. Cini, Controlled release of pilocarpine from coated polymeric ophthalmic inserts prepared by extrusion, Int. J. Pharm. 86 (1992) 159–166, https://doi.org/10.1016/0378-5173(92)90193-6.

[7] Y. Bin Choy, S.R. Patel, J.-H. Park, B.E. McCarey, H.F. Edelhauser, M.R. Prausnitz, Mucoadhesive microparticles in a rapidly dissolving tablet for sustained drug delivery to the eye, Investig. Opthalmology Vis. Sci. 52 (2011) 2627, https://doi.org/10.1167/iovs.10-6465.

[8] I. Ince, E. Karasulu, H. Ates, A. Yavasoglu, L. Kirilmaz, A novel pilocarpine microemulsion as an ocular delivery system : in vitro and in vivo studies, J. Clin. Exp. Ophthalmol. 6 (2015), https://doi.org/10.4172/2155-9570.1000408.

[9] R.P. Brannigan, V.V. Khutoryanskiy, Synthesis and evaluation of mucoadhesive acryloyl-quaternized PDMAEMA nanogels for ocular drug delivery, Colloids Surf. B Biointerfaces 155 (2017) 538–543, https://doi.org/10.1016/j.colsurfb.2017.04.050.

[10] M. Farahmandnejad, S. Alipour, A. Nokhodchi, Physical and mechanical properties of ocular thin films: a systematic review and meta-analysis, Drug Discov. Today 29 (2024) 103964, https://doi.org/10.1016/j.drudis.2024.103964.

[11] M. Tighsazzadeh, J.C. Mitchell, J.S. Boateng, Development and evaluation of performance characteristics of timolol-loaded composite ocular films as potential delivery platforms for treatment of glaucoma, Int. J. Pharm. 566 (2019) 111–125, https://doi.org/10.1016/j.ijpharm.2019.05.059.

[12] G.-H. Hsiue, J.-A. Guu, C.-C. Cheng, Poly(2-hydroxyethyl methacrylate) film as a drug delivery system for pilocarpine, Biomaterials 22 (2001) 1763–1769, https://doi.org/10.1016/S0142-9612(00)00336-7.

[13] H.G. Wafa, E.A. Essa, A.E. El-Sisi, G.M. El Maghraby, Ocular films versus film-forming liquid systems for enhanced ocular drug delivery, Drug Deliv. Transl. Res. 11 (2020) 1084–1095, https://doi.org/10.1007/s13346-020-00825-1.

[14] T.A. Alotaibi, A. Iyire, S. Assaf, E.Z. Dahmash, Development and characterization of niosomes loaded mucoadhesive biodegradable ocular inserts for extended release of pilocarpine HCl, Futur. J. Pharm. Sci. 10 (2024) 22, https://doi.org/10.1186/s43094-024-00598-1.

[15] C. Alexander, Synthetic polymer systems in drug delivery, Expert Opin. Emerg. Drugs 6 (2001) 345–363, https://doi.org/10.1517/14728214.6.2.345.

[16] R. Cazorla-Luna, A. Martín-Illana, F. Notario-Pérez, R. Ruiz-Caro, M.-D. Veiga, Naturally occurring polyelectrolytes and their use for the development of complex-based mucoadhesive drug delivery systems: an overview, Polymers 13 (2021) 2241, https://doi.org/10.3390/polym13142241.

[17] S. Ghosh, Recent research and development in synthetic polymer-based drug delivery systems, J. Chem. Res. (2004) 241–246, https://doi.org/10.3184/030823404120915 8.

[18] M. Harun-Or-Rashid, M.N. Aktar, M.S. Hossain, N. Sarkar, M.R. Islam, M.E. Arafat, S. Bhowmik, S.I. Yusa, Recent advances in micro- and nano-drug delivery systems based on natural and synthetic biomaterials, Polymers 15 (2023), https://doi.org/10.3390/polym15234563.

[19] J. Li, H. Xiang, Q. Zhang, X. Miao, Polysaccharide-based transdermal drug delivery, Pharmaceuticals 15 (2022) 602, https://doi.org/10.3390/ph15050602.

[20] P. Patel, G. Patel, Formulation, ex-vivo and preclinical in-vivo studies of combined ph and ion-sensitive ocular sustained in situ hydrogel of timolol maleate for the treatment of glaucoma, Biointerface Res. Appl. Chem. 11 (2021) 8242–8265, https://doi.org/10.33263/BRIAC111.82428265.

[21] L.E. Agibayeva, D.B. Kaldybekov, N.N. Porfiryeva, V.R. Garipova, R. A. Mangazbayeva, R.I. Moustafine, I.I. Semina, G.A. Mun, S.E. Kudaibergenov, V. V. Khutoryanskiy, Gellan gum and its methacrylated derivatives as in situ gelling mucoadhesive formulations of pilocarpine: in vitro and in vivo studies, Int. J. Pharm. 577 (2020), https://doi.org/10.1016/j.ijpharm.2020.119093.

[22] G.K. Abilova, D.B. Kaldybekov, E.K. Ozhmukhametova, A.Z. Saimova, D. S. Kazybayeva, G.S. Irmukhametova, V.V. Khutoryanskiy, Chitosan/poly(2-ethyl-2-oxazoline) films for ocular drug delivery: formulation, miscibility, in vitro and in vivo studies, Eur. Polym. J. 116 (2019) 311–320, https://doi.org/10.1016/j.eurpolymj.2019.04.016.

[23] M. Preis, K. Knop, J. Breitkreutz, Mechanical strength test for orodispersible and buccal films, Int. J. Pharm. 461 (2014) 22–29, https://doi.org/10.1016/j.ijpharm.2013.11.033.

[24] F.G. Prezotti, I. Siedle, F.I. Boni, I. Müller, B. Stringhetti, F. Cury, Mucoadhesive films based on gellan gum/pectin blends as potential platform for buccal drug delivery, Pharmaceut. Dev. Technol. 25 (2020) 159–167, https://doi.org/10.1080/10837450.2019.1682608.

[25] I.S.M. Noor, S.R. Majid, A.K. Arof, D. Djurado, S. Claro Neto, A. Pawlicka, Characteristics of gellan gum-LiCF3SO3polymer electrolytes, Solid State Ionics 225 (2012) 649–653, https://doi.org/10.1016/j.ssi.2012.03.019.

[26] S.R. Sudhamani, M.S. Prasad, K. Udaya Sankar, DSC and FTIR studies on Gellan and polyvinyl alcohol (PVA) blend films, Food Hydrocolloids 17 (2003) 245–250, https://doi.org/10.1016/S0268-005X(02)00057-7.

[27] P. Yilmaz Erdogan, F.B. Emre, T. Seçkin, Preparation of poly (N-Isopropylacrylamide)-poly(2-ethyl-2-oxazoline) and their self-assembly properties with dicarboxylic acid, J. Turkish Chem. Soc. Sect. A Chem. 11 (2024) 813–824, https://doi.org/10.18596/jotcsa.1150117.

[28] S. Soradech, P. Kengkwasingh, A.C. Williams, V.V. Khutoryanskiy, Synthesis and evaluation of poly(3-hydroxypropyl ethylene-imine) and its blends with chitosan forming novel elastic films for delivery of haloperidol, Pharmaceutics 14 (2022) 2671, https://doi.org/10.3390/pharmaceutics14122671.

[29] A. Astanina, J.T. Koivisto, M. Hannula, T. Salminen, M. Kellomäki, J. Massera, Chemical interactions in composites of gellan gum and bioactive glass: self-crosslinking and in vitro dissolution, Front. Chem. 11 (2023) 1–22, https://doi.org/10.3389/fchem.2023.1133374.

[30] S. Aafrin Hazaana, A. Joseph, S. Selvasekarapandian, R. Meera Naachiyar, M. Vengadesh Krishna, N. Muniraj Vignesh, Development and characterization of biopolymer electrolyte based on gellan gum (GG) with lithium chloride (LiCl) for the application of electrochemical devices, Polym. Bull. 80 (2023) 5291–5311, https://doi.org/10.1007/s00289-022-04316-w.

[31] C. Naveen, M. Muthiah, Investigations on magnesium ion conducting gellan gum-based biopolymer blend electrolytes for energy storage applications, Energy Environ. (2024), https://doi.org/10.1177/0958305X241230621.

[32] M. Yamada, Y. Kametani, Preparation of gellan gum-inorganic composite film and its metal ion accumulation property, J. Compos. Sci. 6 (2022), https://doi.org/10.3390/jcs6020042.

[33] J. Lavikainen, M. Dauletbekova, G. Toleutay, M. Kaliva, M. Chatzinikolaidou, S. E. Kudaibergenov, A. Tenkovtsev, V.V. Khutoryanskiy, M. Vamvakaki, V. Aseyev, Poly (2-ethyl-2-oxazolines) grafted gellan gum for potential application in transmucosal drug delivery, Polym. Adv. Technol. 32 (2021) 2770–2780, https://doi.org/10.1002/pat.5298.

[34] Z.S. Nurkeeva, G.A. Mun, A.V. Dubolazov, Khutoryanskiy, V. V, pH effects on the complexation, miscibility and radiation-induced crosslinking in poly(acrylic acid)-poly(vinyl alcohol) blends, Macromol. Biosci. 5 (2005) 424–432, https://doi.org/10.1002/mabi.200400200.

[35] O.V. Khutoryanskaya, P.W.J. Morrison, S.K. Seilkhanov, M.N. Mussin, E. K. Ozhmukhametova, T.K. Rakhypbekov, V.V. Khutoryanskiy, Hydrogen-bonded complexes and blends of poly(acrylic acid) and methylcellulose: nanoparticles and mucoadhesive films for ocular delivery of riboflavin, Macromol. Biosci. 14 (2014) 225–234, https://doi.org/10.1002/mabi.201300313.

[36] M.R. Snowdon, A.K. Mohanty, M. Misra, Miscibility and performance evaluation of biocomposites made from polypropylene/poly(lactic acid)/Poly(hydroxybutyrate-co-hydroxyvalerate) with a sustainable biocarbon filler, ACS Omega 2 (10) (2017) 6446–6454, https://doi.org/10.1021/acsomega.7b00983.

[37] V.V. Khutoryanskiy, Advances in mucoadhesion and mucoadhesive polymers, Macromol. Biosci. 11 (2011) 748–764, https://doi.org/10.1002/mabi.201000388.